This article was downloaded by: [Institute Of Atmospheric Physics]
On: 09 December 2014, At: 15:30
Publisher: Taylor & Francis
Informa Ltd Registered in England and Wales Registered Number: 1072954 Registered office: Mortimer House, 37-41 Mortimer Street, London W1T 3JH, UK

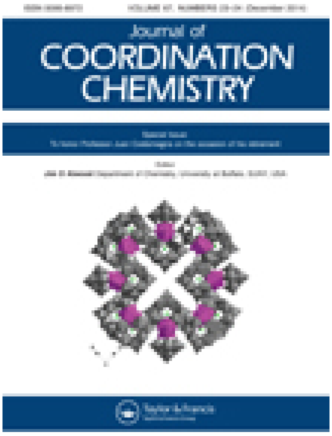

Click for updates

Journal of Coordination Chemistry
Publication details, including instructions for authors and subscription information:
http://www.tandfonline.com/loi/gcoo20

Rhenium and molybdenum poorly crystalline disulfides and their mesophases with hexadecylamine

Juan Antonio Aliaga[ab], Juan Francisco Araya[ab], Roberto Villarroel[ab], Harold Lozano[ab], Gabriel Alonso-Nuñez[c] & Guillermo González[ab]

[a] Department of Chemistry, Faculty of Sciences, Universidad de Chile, Santiago, Chile
[b] Center for Development of Nanoscience and Nanotechnology, CEDENNA, Santiago, Chile
[c] Center of Nanoscience & Nanotechnology, Universidad Nacional Autónoma de México, Ensenada, Mexico

Accepted author version posted online: 24 Oct 2014.Published online: 30 Oct 2014.

To cite this article: Juan Antonio Aliaga, Juan Francisco Araya, Roberto Villarroel, Harold Lozano, Gabriel Alonso-Nuñez & Guillermo González (2014) Rhenium and molybdenum poorly crystalline disulfides and their mesophases with hexadecylamine, Journal of Coordination Chemistry, 67:23-24, 3884-3893, DOI: 10.1080/00958972.2014.975220

To link to this article: http://dx.doi.org/10.1080/00958972.2014.975220

PLEASE SCROLL DOWN FOR ARTICLE

Taylor & Francis makes every effort to ensure the accuracy of all the information (the “Content”) contained in the publications on our platform. However, Taylor & Francis, our agents, and our licensors make no representations or warranties whatsoever as to the accuracy, completeness, or suitability for any purpose of the Content. Any opinions and views expressed in this publication are the opinions and views of the authors, and are not the views of or endorsed by Taylor & Francis. The accuracy of the Content should not be relied upon and should be independently verified with primary sources of information. Taylor and Francis shall not be liable for any losses, actions, claims, proceedings, demands, costs, expenses, damages, and other liabilities whatsoever or howsoever caused arising directly or indirectly in connection with, in relation to or arising out of the use of the Content.

Journal of Coordination Chemistry, 2014
Vol. 67, Nos. 23–24, 3884–3893, http://dx.doi.org/10.1080/00958972.2014.975220

Rhenium and molybdenum poorly crystalline disulfides and their mesophases with hexadecylamine

JUAN ANTONIO ALIAGA†‡, JUAN FRANCISCO ARAYA†‡, ROBERTO VILLARROEL†‡, HAROLD LOZANO†‡, GABRIEL ALONSO-NUÑEZ§ and GUILLERMO GONZÁLEZ*†‡

†Department of Chemistry, Faculty of Sciences, Universidad de Chile, Santiago, Chile
‡Center for Development of Nanoscience and Nanotechnology, CEDENNA, Santiago, Chile
§Center of Nanoscience & Nanotechnology, Universidad Nacional Autónoma de México, Ensenada, Mexico

(*Received 1 July 2014; accepted 1 October 2014*)

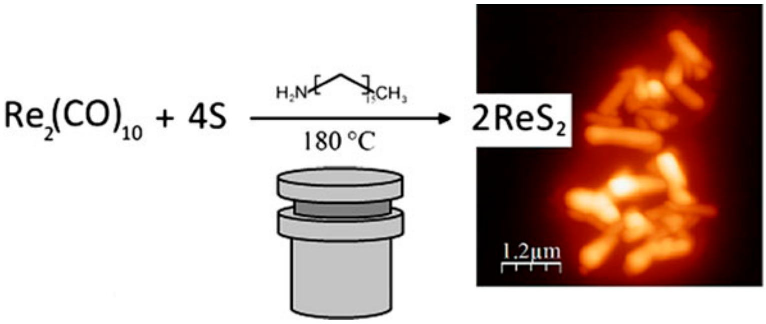

Sulfides of molybdenum and rhenium poorly crystalline were prepared by solvothermal oxidative decarbonylation of the respective metal carbonyls with sulfur using *p*-xylene as solvent. The same reaction, but in presence of hexadecylamine (HDA), was used for preparing the nanocomposites MoS_2/HDA and ReS_2/HDA. The products were analyzed by X-ray diffraction analysis, scanning electron microscopy, atomic force microscopy, and Fourier-transform infrared spectroscopy. The products, MoS_2 and ReS_2, are structurally similar but morphologically different: small undefined particles (150–300 nm) and well-defined, almost perfect microspheres (0.4–2.8 µm), respectively. Preparations containing HDA lead to the corresponding layered nanocomposites. MoS_2/HDA is a dark solid easily separable from the reaction mixture, while ReS_2/HDA remains as a suspension in *p*-xylene, from which it is obtained by evaporating the solvent under vacuum. Both are layered species with basal spacing of 33.8 Å (Mo) and 30.4 Å (Re), respectively. The preparation of thin films of ReS_2/HDA from its suspension by evaporating the solvent in the air produces small cylindrical particles of about 0.4 × 1.0 µm in size. Differences in the behavior of Mo and Re derivatives are discussed considering the coordination of the metal and the electronic structures of both metal disulfides.

Keywords: Amorphous materials; Composite materials; Rhenium sulfide; Molybdenum sulfide

---

*Corresponding author. Email: ggonzale@uchile.cl

1. Introduction

Transition metal sulfides (TMS) MS_2 like those of molybdenum and rhenium have layered graphite-like structures, with S–M–S layers stacked in the direction perpendicular to the layer plane by van der Waals forces [1]. Due to this special structure, these products can easily provide active sites and high specific surface areas, particularly when they are poorly crystalline phases or nanostructured [2]. These compounds, especially MoS_2, have been subject of numerous applications in lithium batteries [3], lubricants [4, 5], hydrogen storage [6], or as catalysts for hydrodesulfurization and hydrodenitrogenation of crude petroleum [7]. In this latter field, ReS_2 has proved to be a very active catalyst, even better than MoS_2 [8]. The possibility of incorporating foreign atoms, molecules, or ions between the layers for producing a diversity of intercalation compounds to form new materials is also an interesting property of this kind of structure.

The intercalation of donor species into MoS_2, particularly of amines, is well known [9]. However, due to the inertness of the most stable crystalline form of this sulfide, 2H-MoS_2, most intercalation products have to be prepared by exfoliation of Li_xMoS_2 in water [10]. Such a procedure induces higher reactivity due not only to the physical effect of producing smaller aggregates or even single MS_2 layers, but also to an alteration of the electronic structure of the layers, mainly generated by a change of the geometry of the coordination sphere of molybdenum in the MoS_6 unit, from trigonal prismatic to octahedral [9]. That notwithstanding, intercalation of dodecylamine into molybdenum disulfide has been also attained in the production of MoS_2 by oxidative decarbonylation of $Mo(CO)_6$ with elemental sulfur using the amine both as solvent and as template [11]. Such a decarbonylation reaction, but without any template, is a successful method for obtaining the poorly stacked sulfides of MoS_2 and ReS_2, either in bulk [12, 13] or embedded in carbonaceous composites [14, 15]. Recently, we have also experienced that the morphology of the ReS_2/C composites obtained by this reaction may be in some extent modulated by selecting the solvent [16].

In this work, we compare the morphology of the products obtained by the solvothermal oxidative decarbonylation of neutral carbonyls of Mo and of Re with sulfur, using *p*-xylene as solvent, as well as of those attained from these same reactions performed in presence of hexadecylamine (HDA). In absence of the amine, molybdenum disulfide microparticles with undefined shape are obtained, while rhenium disulfide particles show an almost perfect spherical morphology, thus pointing to a particular catalytic effect of this sulfide on the decomposition of the solvent. The presence of the amine induces the formation of typical layered MS_2/amine nanocomposites. Contrasting with its Mo analog, the ReS_2 nanocomposite is directly obtained as very stable *p*-xylene suspensions from which bulk solids with morphologies which depend on the method used for eliminating the solvent are separated.

2. Experimental procedure

0.3 mM of $Re_2(CO)_{10}$ analytically pure (Sigma-Aldrich 98%), 6.0 mM of sulfur powder (Sigma-Aldrich 99.8%) and about 8 mL of *p*-xylene (Sigma-Aldrich 99%) were put into a 10 mL Teflon-lined autoclave, heated at 180 °C in an electrical oven for 24 h and then cooled naturally. A black powder suspension was obtained. The product was separated by centrifugation, washed with diethyl ether, filtered, and dried at vacuum for 10 h, getting a black powder, labeled as ReS_2. The same solvothermal procedure was repeated using 0.3 mM of $Re_2(CO)_{10}$, 1.2 mM of sulfur powder, 8 mL of *p*-xylene, and 0.3 mM of HDA.

The product of reaction was a black-reddish oily suspension superstable, which remains unaltered for more than six months. After evaporating the solvent under active vacuum at 50 °C for three days, a black shiny solid was obtained, labeled as ReS_2/HDA.

The same procedure above was used for preparing analogous molybdenum derivatives. The solvothermal treatment of 0.7 mM of $Mo(CO)_6$ (Sigma-Aldrich 99.9%), 1.4 mM of sulfur powder (Sigma-Aldrich 99.8%), and about 8 mL of *p*-xylene (Sigma-Aldrich 99%) leads to formation of a black powder. The same reaction was repeated using the same amounts of reagents and solvent, but adding 0.7 mM of HDA. A black precipitate which contrasts the ReS_2 nanocomposite was easily separable by centrifugation.

Bulk solid products were characterized by powder X-ray diffraction (XRD) analysis, performed with a SIEMENS D5000 powder diffractometer with CuKα radiation ($k = 1.54060$ Å) at 30 mA and 40 kV; scanning electron microscopy (SEM), SEM LEO 1420VP, Oxford Instruments; Fourier-transform infrared (FT-IR) spectra (4000–500 cm^{-1}) recorded in a Bruker IFS 25 model infrared spectrophotometer using diluted samples in KBr disks; and atomic force microscopy (AFM) topography images obtained using a NT-MDT NTEGRA PRIMA SPM, obtained in semi-contact mode with 300 kHz Si probes.

Thin films of ReS_2 nanocomposite from the as-prepared suspension for SEM observations were obtained by drop casting of the dilute suspension onto a copper lamina; for AFM measurements the samples diluted in *p*-xylene were spin coated (2000 rpm) onto mica substrates.

3. Results

The synthesis of MoS_2 and ReS_2 by solvothermal oxidative decarbonilation of Mo and Re carbonyls with sulfur using *p*-xylene as solvent leads to formation of the corresponding metal disulfides. XRD patterns of molybdenum and rhenium sulfides prepared by this procedure are shown in figure 1. The DRX pattern of ReS_2 depicted in figure 1a is consistent

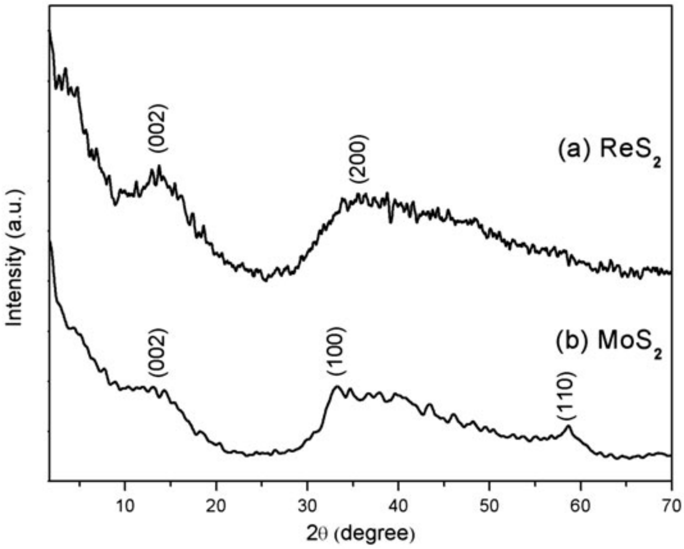

Figure 1. XRD patterns of as-prepared (a) rhenium sulfide and (b) molybdenum sulfide synthesized at 180 °C in *p*-xylene.

with the expected one for a poorly crystalline ReS_2 triclinic phase with unit cell parameters $a = 6.417(4)$, $b = 6.377(4)$, $c = 6.461(4)$ (JCPDS 89-0341). The broad (002) reflection centered at $2\theta = 13.4°$ is indicative of small size crystallites and texture effects. The protruding DRX profile in the 2θ range 31–50° arises from the superposition of a series of broad peaks, among them the reflections (2 0 0), (0 3 0) and (0 0 6). The observed DRX pattern matches well with those observed for ReS_2 colloidal particles [17] and fullerene-like IF-ReS_2 [13]. The DRX pattern of the molybdenum sample mainly shows two broadened reflection profiles, centered at $2\theta = 14°$ and 39°, respectively, which are consistent with indexation of the hexagonal MoS_2 with lattice constants $a = 3.161$ Å and $c = 12.299$ Å (JCPDS 37-1492) [18]. The broad Bragg-reflection (0 0 2) at 2θ about 14° is characteristic of a poorly stacked 2H-MoS_2 layered phase, while the protruded profile in the range 30–48° corresponds to the collective exhibition of several reflections; among them those corresponding to the planes (1 0 0), (1 0 1) and (1 0 3). Moreover, the reflection (1 1 0) is detected at $2\theta = 58°$.

The morphology of the as-prepared samples of both metal sulfides (ReS_2 and MoS_2) is compared in figure 2. While the SEM image of MoS_2 shows an irregular granular morphology [figure 2(a)], ReS_2 is obtained as spherically shaped particles [figure 2(b)]. The rhenium sulfide microspheres are smooth and have diameters in the range 0.4–2.8 μm. Molybdenum sulfide particles are, in turn, much smaller with diameters ranging between 150 and 300 nm.

Considering the well-known tendency of layered TMS for intercalating donor species, for instance, alcohols, amines, and particularly, amine-based surfactants, the preparation of MoS_2 and ReS_2 by solvothermal oxidative decarbonylation reactions described earlier was also performed in the presence of HDA. In spite of chemical and structural similitude of both products, the reaction mixtures obtained after the solvothermal treatment of both carbonyls are very different. In the case of molybdenum (MoS_2/HDA), a black precipitate is obtained, easily separable from the solvent (*p*-xylene) by centrifugation. A SEM image of this product is shown in figure 3(a). Contrastingly, the reaction with rhenium carbonyl leads to a very stable oily emulsion which remains unaltered for months. From the latter may be obtained a solid product but only after evaporating the solvent under active vacuum (ReS_2/HDA). A SEM image of this bulk solid can be seen in figure 3(b).

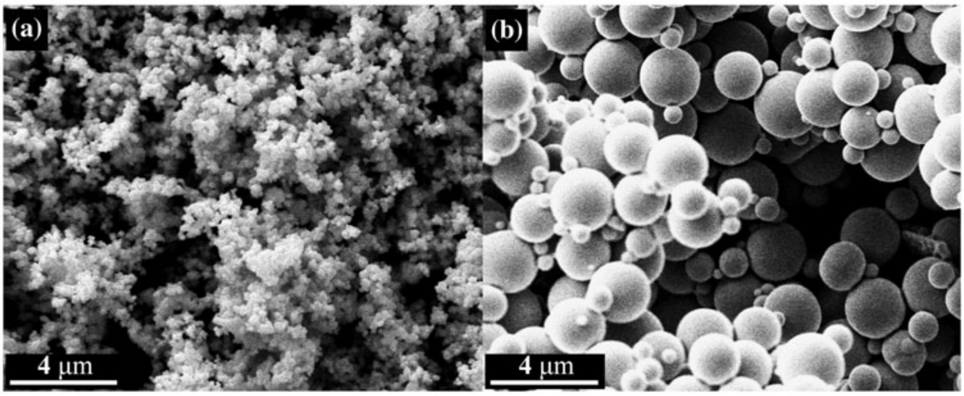

Figure 2. SEM images of samples obtained at 180 °C: (a) MoS_2 and (b) ReS_2.

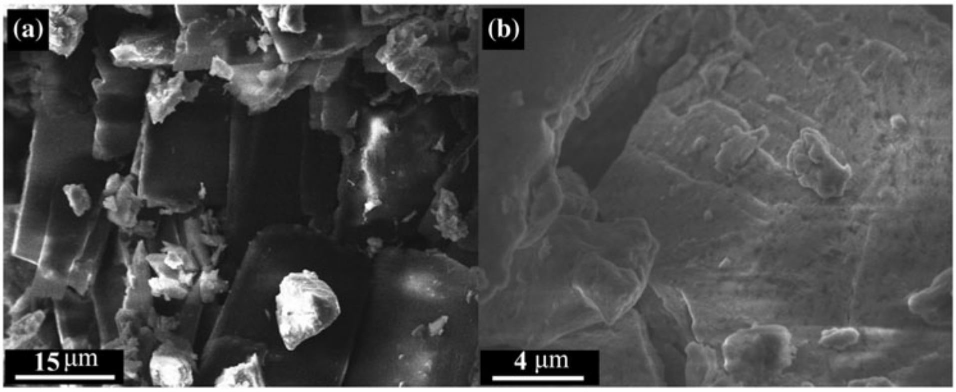

Figure 3. SEM images of composites obtained at 180 °C: (a) MoS_2/HDA and (b) ReS_2/HDA after active vacuum solvent extraction.

XRD patterns of the products obtained in presence of HDA, illustrated in figure 4, reveal that in both cases there is at least a (0 0 l) Bragg reflection at low angles, a feature typical of intercalated layered nanocomposites [1, 19]. The low angle reflections most relevant in the pattern of the MoS_2-based product [figure 4(a)] at $2\theta = 2.61$ and 7.97° may be indexed as corresponding to the (0 0 1) and (0 0 3) crystal planes. From them an interlaminar distance of about 33.8 Å is inferred. This value is similar to that observed by Vanchura *et al.* [11] for a MoS_2/amine intercalate obtained through a reaction similar to that discussed here,

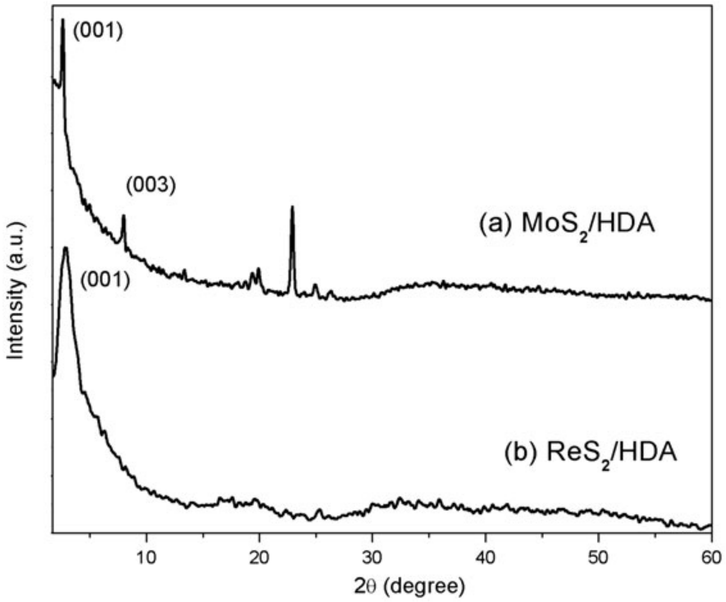

Figure 4. XRD patterns of as-prepared rhenium and molybdenum sulfide composites synthesized at 180 °C in *p*-xylene in presence of HAD: (a) MoS_2/HDA and (b) ReS_2/HDA.

but using the same amine instead of a conventional solvent. Since the basal spacing in these compounds is near to that of a surfactant double layer, the nature of these nanocomposites could be rationalized in a first approximation by applying a geometrical modeling as frequently done for analyzing this kind of nanocomposite, namely considering that these MoS_2/HDA composites in bulk arise from stacking single, MoS_2 layers flanked on both sides by a self-assembled monolayer (SAM) of surfactant molecules. Such a representation is formally equivalent to the intercalation of a surfactant double layer into the interlaminar space of the layered metal sulfide. There, the interlaminar distance is determined by the length of surfactant hydrocarbon chain and the orientation of the long molecular axis of the latter with respect to the surface of the inorganic sheet. The stability of the nanocomposites principally depends on two variables, namely the interaction of the polar head of the surfactant with the host and, often in important amount, by the van der Waals interactions between hydrocarbon tails of the surfactant. Therefore, actual interlaminar distance and the degree of order in such structures depend on the possibility of optimizing these variables.

The XRD pattern observed for the composite of ReS_2/HDA is qualitatively similar to that of MoS_2/HDA just discussed. There is a Bragg peak at $2\theta = 2.9°$ which would correspond to the plane (0 0 l) and an interlaminar distance of about 30.4 Å [figure 4(b)]. However, this broad diffraction peak is practically the sole relevant in this diffractogram, thus pointing to a layered product, but more poorly stacked than the MoS_2/HDA. Indeed, the average thickness of the particles estimated by the Scherrer formula using the reflection (0 0 l) in the DRX pattern of the rhenium nanocomposite accounts approximately to two layers/particle, while the average thickness of the MoS_2/HDA crystallites measured by the same method indicates an average value of approximately 20 layers/particle. This is in line with the relatively lower crystallinity of the rhenium sulfide commented before.

The presence of amine in the hybrid product ReS_2/HDA was corroborated by analyzing the FT-IR spectrum of the sample. This analysis was also useful for identifying the type of carbonaceous materials formed during the solvothermal reaction, which, according to some previous results [Aliaga *et al.*] appear to be involved in the formation of ReS_2 microspheres in this kind of reaction. The two characteristic bands arising from the symmetric and asymmetric stretching vibration modes of the CH_2 groups in amines are observed at 2851 and 2922 cm^{-1}, respectively. A series of stretching vibrations of N-H bonds with different degree of association appears to give a broad, low intensity band in the range 3500–3000 cm^{-1}, probably together with aromatic-C–H absorptions (*vide infra*). The N–H deformation vibrations, which are observed as an absorption relatively strong at 1636 cm^{-1} and a medium weak one at 901 cm^{-1}, also point to hydrogen-bonded NH_2 groups. The amine-C–N stretching vibration is assigned to a broad peak of medium intensity at 1092 cm^{-1}. In addition to the absorption IR spectrum of HDA, also detected are a series of bands which agree well with many of those in spectra of the poly(*p*-xylylene (PPX) described in the literature [20]. The stretching C–C vibration in the aromatic-ring is observed at 1454 cm^{-1}, while the ring deformation vibrations, in plane and out of plane, are detected at 608 and 500 cm^{-1}, respectively. The frequencies of the aromatic ring C–H deformation vibrations, in and out of plane, are observed at 1030 and 804 cm^{-1}, respectively. The spectrum also shows two well-defined peaks at 2023 and 1911 cm^{-1} which are assignable to rhenium carbonyl. This is indicative that in spite of careful washing of sample, part of the unreacted metal precursor remained trapped in the matrix nanocomposite/PPX.

In addition to the separation of bulk ReS_2 nanocomposite by vacuum drying, the preparation of thin films by evaporating the solvent in air was also attained. Films were deposited by dispersing/drying a few drops of the dilute suspension in *p*-xylene upon substrates

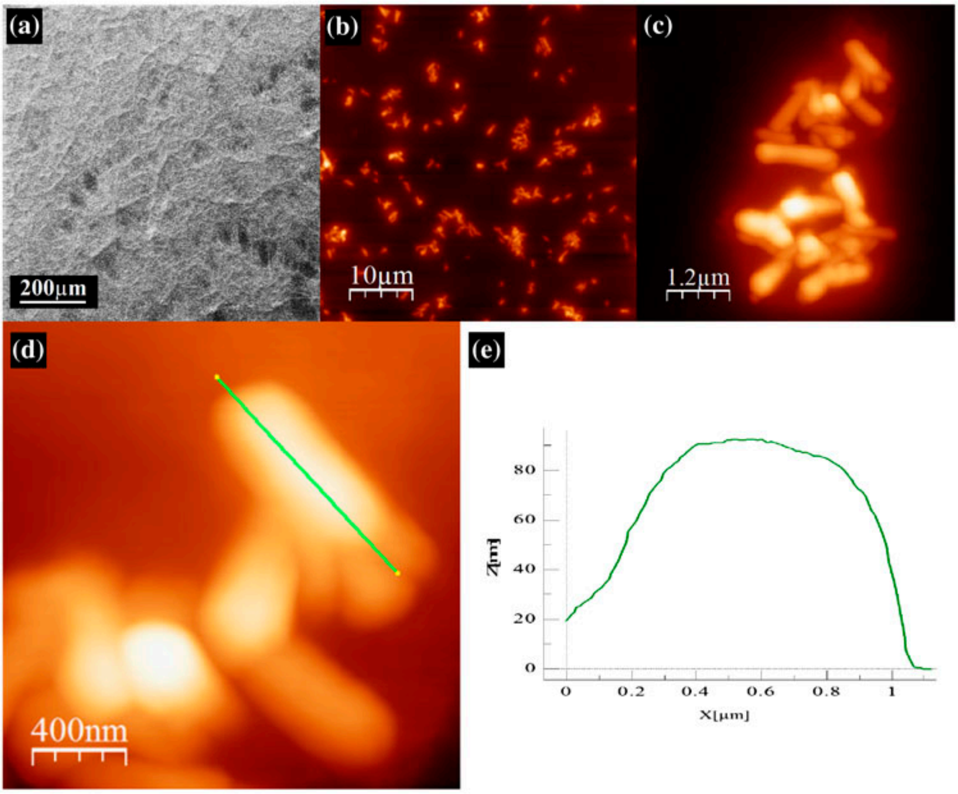

Figure 5. ReS_2 nanocomposites: (a) SEM dendritic morphology, (b)–(c) AFM of sonicated suspension, (d) detail of (c), and (e) cross section analysis of (d).

appropriate for either SEM or AFM analysis. As observed in the SEM image in figure 5(a), the deposit performed without sonication is mainly formed by dendritic agglomerations but neither lamellas nor spheres were detected. A better approach to observe the morphology of these particles is AFM. A series of AFM micrographs of films deposited by spin coating are illustrated in figure 5(b)–(d). In spite of the relatively high dilution of the pristine suspension, tiny agglomerates like those illustrated in figure 5(c) were always observed. However, deposits obtained from the same suspension, but sonicated previously for about 45 min, permit to detect [figure 5(d)] that these agglomerates are mainly formed by small cylindrical particles with diameters around 0.4 μm and about 1 μm in length.

4. Discussion

The solvothermal oxidative decarbonylation of both molybdenum and rhenium carbonyls with sulfur, using *p*-xylene as solvent, is an appropriate strategy for obtaining the corresponding disulfides. Although the products often are not pure phases, have imprecise stoichiometries and/or produce composites with carbonaceous species not well defined, they always have the property of being poorly crystalline layered disulfides, and therefore potentially useful as heterogeneous catalysts [2]. However, in spite of many similarities, the morphology of resulting sulfides is different: MoS_2 is obtained as small particles while ReS_2 almost quantitatively produces well-formed spherical microstructures. This appears to be an effect of the solvent. Indeed, as discussed in a recent study on the effect of the solvent upon this type of reactions to be published elsewhere [16], the formation of spherical shaped products occurs preferentially in systems in which the reaction medium includes solvents or reactants that may be transformed into amphiphilic species able to produce micelle-like aggregates. Although aromatic solvents like *p*-xylene do not belong to this class of solvents, we do hypothesize that the structuration of spheres relies on the formation of PPX during the reaction. Results indicate that this rarely occurs in the case of ReS_2. Contrastingly all attempts to detect this polymer in the preparation of MoS_2 failed. This fact could be a reasonable point to explain the different morphology of both products, corroborating moreover our hypothesis about the particular ability of ReS_2 to catalyze the polymerization of *p*-xylene at relatively low temperatures.

As expected, the presence of HDA in the oxidative decarbonylation of $Re_2(CO)_{10}$ with sulfur, similar to that of $Mo(CO)_6$, leads to formation of a nanocomposite in which the amine appears to be located in the interlaminar space of the layered ReS_2. However, contrary to the case of MoS_2/HDA nanocomposite, which is insoluble in the reaction medium [figure 2(d)], the ReS_2/amine derivative remains as a rather stable suspension. This points to a relatively low reticular energy, agreeing with its poor layer stacking capability.

The peculiarities of the ReS_2/amine nanocomposite described here highlight the influence of the procedures used for its separation on the morphology of the solid. A fast elimination of solvent leads to a cylindrical morphology, e.g. thin films [figure 5(b) and (e)], while with an evaporation of the solvent slower (vacuum) produce lamellae [figure 3(a)]. These results can be rationalized in a first approximation by considering two fundamental aspects involved in these systems, namely differences in the electronic structure of both Mo and Re sulfides and the amphiphilic properties of the HDA.

Recently Tongay *et al.* [21] reported an interesting comparative analysis of the electronic and atomic structures of these two sulfides. Both solids are lamellar structures, consisting in a stack of nearly planar layers formed by metal and sulfur atoms joined by covalent ionic bonds relatively strong. However, they differ in the coordination geometry of the metal atom as well as in the interaction between the metal centers. In 2H-MoS_2, the most stable form of this sulfide, the layers are formed by independent MoS_6 units in which the metal has trigonal-prismatic coordination, while in rhenium sulfide the metal has an octahedral coordination distorted by the formation of a Re–Re bond between neighboring ReS_6 units [8]. The latter entails a different electronic distribution resulting in a lower polarity within the ReS_2 sheet. This eventually leads to a minimization of the van der Waals interactions between the layers to an extent that according to these authors, the behavior of bulk ReS_2 in the bulk would be similar to that of a single sheet [21].

Small reticular energies and high degree of disorder observed for ReS_2 and ReS_2/amine are in line with the minimal interaction between the layers observed in bulk ReS_2 already commented. The low polarity inside ReS_2 sheets also makes the interaction with donors like amines relatively weak thus avoiding the formation of densely packed SAMs. Although such effects can explain the different solubility of Mo and Re products, this appears to be not enough to understand neither the stability of the ReS_2 suspension nor the dependence of the morphology of the products of the procedure used for eliminating the solvent. As mentioned above, these systems have to be also analyzed by considering the self aggregation of the surfactant in the reaction medium.

The micelle behavior of simple surfactants like HDA may be described in a reasonably satisfactory approach, taking into account the effective molecular dimensions of the surfactant molecule in the medium; for instance using the "critical packing parameter," R ($R = v/(a_0\ l_c)$, where v is the volume of the hydrocarbon chains, a_0 the optimal head-group area, and l_c the critical chain length) [22]. Linear amphiphilic species with values of R near to 1 (cylindrical-shaped effective geometry), in general tend to form laminar aggregates, while those with conical shapes –R values greater or lower than 1– shall form aggregates with different degrees of curvature. The value of R for HDA, which in water is near one, is drastically reduced in a nonpolar medium due to solvation of the hydrocarbon chain, so it is expected that in *p*-xylene this surfactant will form inverse micelles. Therefore, it is very probable that the reaction of the metal carbonyl with sulfur occurs within these micelles. In the case of molybdenum sulfide, the layers have relatively high polarity being thus able to interact with surfactant polar heads. The higher this interaction the more effective will be the segregation of solvent from the amine. This causes a reduction of the critical packing parameter of the surfactant, thus increasing its tendency to form laminar double layer aggregates. Such supramolecular structures became further stabilized by interacting with metal sulfide layers, producing finally the precipitation of the nanocomposite. In the case of ReS_2, the low polarity and scarce stacking ability of this compound avoid the segregation of the solvent from the amine, remaining unaltered the inverse micelles already commented. Thus, the sulfide encapsulated in such aggregates remains as a stable suspension in the reaction medium. However, during the drying process under active vacuum, the solvent is forced to evaporate from the suspension, thus inducing an increment of the concentration of the surfactant until a point allowing the formation of a layered nanocomposite. This leads to a solid which is similar to the molybdenum derivative but more disordered. A slow evaporation of solvent at normal atmospheric pressure, as that occurring in the formation of the thin films described before, appears to stabilize an intermediate situation in which quasi-cylindrical surfactant micelles are formed. These aggregates would act as templates for generating the nanocomposites with the worm-like morphology of the particles observed in figure 5(d) and (e).

5. Conclusion

Molybdenum and rhenium sulfides as well as their nanocomposites with HDA have been synthesized by oxidative decarbonylation of molybdenum and rhenium carbonyls with elemental sulfur under solvothermal conditions. In all the cases, poorly stacked layered products are obtained. However, the morphology of the products, particularly the degree of order in their solids, is different.

The products of the synthesis of molybdenum sulfide and of its nanocomposite with HDA prepared under the reaction conditions described here are similar to other poorly crystalline solids obtained by a variety of different methods. This procedure is also excellent for easy obtaining of poorly crystalline ReS_2 in the form of almost perfect spherical aggregates. ReS_2, like molybdenum and other transition metal disulfides, is also able to produce layered nanocomposites by intercalation of amphiphilic species like HDA. In this particular case, moreover, the morphology of the product could be modulated not only by the nature of the surfactant but also by selecting the strategy used for separating the solid products from the reaction mixture.

Differences observed between the sulfides and their nanocomposites with HDA of molybdenum and rhenium appear to correlate with their coordination geometries in these compounds. Different to the trigonal-prismatic coordination of MoS_2, rhenium has an octahedral coordination sphere which is distorted due to a Re–Re bond between ReS_6 neighboring units. This makes its properties somewhat atypical. For instance, a rather low polarity inside each layer, that affects the interlayer interactions; this, up to the extreme that bulk ReS_2 can behave like a single sheet [21]. Main results discussed in this work – solids with depressed stacking ability, the low affinity for donor species and morphological dependence of strategies for synthesis and separation of the solids – are good examples of peculiarities of the chemistry of rhenium disulfide.

Considering the potentiality of rhenium disulfide for diverse applications including heterogeneous catalysis, further studies for testing the relevance of preparation procedures described here are in course.

Funding

This research was partially funded by FONDECYT (Contracts 1131112), Basal Financing Program CONICYT, FB0807 (CEDENNA), Millennium Science Nucleus P010-061-F, and CONICYT for PhD fellowship.

References

[1] N. Mirabal, V. Lavayen, E. Benavente, M.A. Santa Ana, G. Gonzalez. *Microelectron. J.*, **35**, 37 (2004).
[2] G. Alonso, G. Berhault, A. Aguilar, V. Collins, C. Ornelas, S. Fuentes, R.R. Chianelli. *J. Catal.*, **208**, 359 (2002).
[3] H. Hwang, H. Kim, J. Cho. *Nano Lett.*, **11**, 4826 (2011).
[4] Z. Xiaodong, F. Xun, S. Huaqiang, H. Zhengshui. *Lubr. Sci.*, **19**, 71 (2007).
[5] J. Tannous, F. Dassenoy, I. Lahouij, T. Le Mogne, B. Vacher, A. Bruhács, W. Tremel. *Tribol. Lett.*, **41**, 55 (2011).
[6] L. Ye, C. Wu, W. Guo, Y. Xie. *Chem. Commun.*, **45**, 4738 (2006).
[7] G. Alonso, M.H. Siadati, G. Berhault, A. Aguilar, S. Fuentes, R.R. Chianelli. *Appl. Catal. A: Gen.*, **263**, 109 (2004).
[8] N. Escalona, M. Vrinat, D. Laurenti, F.J. Gil Llambias. *Appl. Catal. A: Gen.*, **322**, 113 (2007).
[9] E. Benavente, M.A. Santa Ana, F. Mendizabal, G. Gonzalez. *Coord. Chem. Rev.*, **224**, 87 (2002).
[10] N.D. Lenenko, E.N. Semina, V.I. Zaikovskii, A.S. Golub. *Mater. Chem. Phys.*, **141**, 35 (2013).
[11] B.A. Vanchura, P. He, V. Antochshuk, M. Jaroniec, A. Ferryman, D. Barbash, J.E. Fulghum, S.D. Huang. *J. Am. Chem. Soc.*, **124**, 12090 (2002).
[12] D. Duphil, S. Bastide, C. Lévy-Clément. *J. Mater. Chem.*, **12**, 2430 (2002).
[13] A. Yella, H.A. Therese, N. Zink, M. Panthöfer, W. Tremel. *Chem. Mater.*, **20**, 3587 (2008).
[14] V.G. Pol, S.V. Pol, P.P. George, A. Gedanken. *J. Mater. Sci.*, **43**, 1966 (2008).
[15] V.G. Pol, S.V. Pol, N. Perkas, A. Gedanken. *J. Phys. Chem. C*, **111**, 134 (2007).
[16] J.A. Aliaga, J.F. Araya, H. Lozano, E. Benavente, G. Alonso-Nuñez, G. González, An easy one-pot solvothermal synthesis of poorly crystalline solid ReS_2/C microspheres, 2014. Submitted May 2014.
[17] W. Tu, B. Denizot. *J. Colloid Interface Sci.*, **310**, 167 (2007).
[18] Q. Wang, J. Li. *J. Phys. Chem. C*, **111**, 1675 (2007).
[19] E. Escalona Platero, F. Ruiz de Peralta, C. Otero Areán. *Catal. Lett.*, **34**, 65 (1995).
[20] P. Simon, S. Mang, A. Hasenhindl, W. Gronski, A. Greiner. *Macromolecules*, **31**, 8775 (1998).
[21] S. Tongay, H. Sahin, C. Ko, A. Luce, W. Fan, K. Liu, J. Zhou, Y.-S. Huang, C.-H. Ho, J. Yan, D.F. Ogletree, S. Aloni, J. Ji, S. Li, J. Li, F.M. Peeters, J. Wu. *Nat. Commun.*, **5**, 3252 (2014).
[22] J. Zhang, Z.L. Wang, J. Liu, S. Chen, G.Y. Liu. In *Nanostructure Science and Technology*, D.J. Lockwood (Ed.), Chap. 2, pp. 17–20, Kluwer Academic, New York (2004).